Peroxy Radical Probe for Motion in Poly(tetrafluoroethylene) Chains

Darbha Suryanarayana,[†] Larry Kevan,*[†] and Shulamith Schlick[‡]

Contribution from the Departments of Chemistry, University of Houston, Houston, Texas 77004, and University of Windsor, Windsor, Ontario N9B 3P4, Canada. *Received June 15, 1981*

Abstract: The temperature dependences in the Q-band electron-spin resonance (ESR) spectra of mid-chain and end-chain peroxy radicals in γ-irradiated poly(tetrafluoroethylene) are investigated experimentally and theoretically, using modified Bloch equations. Computer simulations are carried out for the following motional models: cubic jump, C–O bond rotation (120° and 180° jumps), and chain axis rotation (90° and 120° jumps). For the mid-chain peroxy radical [$-CF_2CF(OO\cdot)-CF_2$], the partial g averaging in the ESR spectra could be fit well by chain axis rotation with 90° jumps, whereas the complete g averaging observed at room temperature for the end-chain peroxy radical [$-CF_2-CF_2-CF_2(OO\cdot)$] could be fit using a cubic jump model. An activation energy of 18.4 kJ/mol was found for the mid-chain peroxy-radical motion and 11.2 kJ/mol for the end-chain peroxy-radical motion.

Nitroxide radicals have been widely used to study molecular motion in various systems by analysis of the incomplete averaging of the hyperfine anisotropy.[1] The maximum hyperfine anisotropy is ~70 MHz so motions characterized by reorientation times up to $\sim 1 \times 10^{-8}$ s may induce spectral changes.

Schlick and Kevan[2-4] have recently shown that peroxy radicals are also effective probes for studing molecular motion in solids by incomplete averaging of their g anisotropy. The maximum g anisotropy corresponds to ~200 MHz which means that the peroxy spectra are potentially sensitive to faster motions up to 5×10^{-9} s than are nitroxide spectra. Peroxy probes have the advantage that peroxy conversion of intrinsic radicals can often be accomplished by simple exposure to air or oxygen at room temperature. The analysis of the temperature dependence of peroxy-radical electron-spin resonance (ESR) spectra has indicated that the peroxy spectra are more sensitive to the motional model than are nitroxide spectra so that *specific* motional mechanisms can often be deduced if the ESR spectra are studied over the *entire* temperature range between the rigid limit and high-temperature extremes. The utility of peroxy-radical probes for this purpose has been demonstrated for (triphenylmethyl)peroxy radicals in γ-irradiated triphenylacetic acid,[2] $(CO_2-O_2)^-$, on a magnesium oxide surface[3] and peroxypolyethylene radicals in a urea–polyethylene complex.[4]

Recent studies by Freed and co-workers have also shown that VO^{2+} complexes in aqueous and organic solutions[5] and O_2^- adsorbed on Ti^{4+} supported on porous Vycor glass[6] are also useful motional probes which are particularly sensitive to specific motional mechanisms.

Peroxy-radical probes seem potentially useful for the study of motions in polymers and particularly for assessing the role of motion in photo-oxydegradation mechanisms. In this study we report results on two different peroxy radicals formed in poly(tetrafluoroethylene) (PTFE) and are able to deduce probable specific motional mechanisms.

The radicals formed by high-energy irradiation of PTFE at room temperature have been widely studied.[7-18] Mid-chain radicals (I) and end-chain or propagating radicals (II) have been identified.[7,8] After exposure to oxygen these radicals readily convert to the corresponding peroxy radicals III and IV.[8] ESR spectra of these peroxy radicals exhibit significant variation in their line-shapes with temperature.[15] In the rigid limit at 77 K the ESR spectra of III and IV have the same g anisotropy $g_\parallel = 2.038$ and $g_\perp = 2.002$. Different motional averaging occurs for III and IV at room temperature leading to a partial g anisotropy averaging such that $g_\perp > g_\parallel$ for III and complete g anisotropy averaging to give g_{iso} for IV.[17]

Ovenall[12] followed by Iwasaki and Sakai[15] and more recently by Olivier, Marachi, and Che[17,18] have interpreted the temperature-dependent ESR spectra in terms of polymer chain axis rotation. In these previous studies only the room temperature and rigid limit spectra have been analyzed, using relations such as those given by Toriyama and Iwasaki.[19]

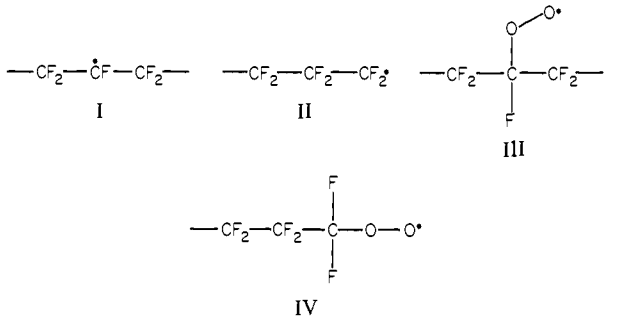

Here we measure the ESR spectra of III and IV over the entire temperature range and simulate the results for different specific motional mechanisms. For the mid-chain peroxy radical III the most probable motional mechanism is chain axis rotation via 90° jumps and for the end-chain peroxy radical IV a cubic jump mechanism is indicated.

Experimental Section

Powdered poly(tetrafluoroethylene) in Pyrex tubes was evacuated to 10^{-4} torr at 100 °C for about 96 h. The tubes were sealed under vacuum and were γ-irradiated in a Gammacell 200 ^{60}Co γ-source (Atomic Energy of Canada, Ltd.) at room temperature at a dose rate of 1.93 Mrad h^{-1} to a total dose of about 300 Mrad. The irradiated samples were annealed at 200 °C for about 0.7 h to destroy the end-chain radical (II) to a greater extent than the mid-chain radical (I). The tubes were then opened and oxygen introduced to produce mainly the peroxy mid-chain radical (III). In order to selectively prepare only the end-chain peroxy

[†] University of Houston.
[‡] University of Windsor.

(1) Berliner, L., Ed. "Spin Labeling: Theory and Application"; Academic Press: New York, 1976; Vol. 1.
(2) Schlick, S.; Kevan, L. *J. Phys. Chem.* **1979**, *83*, 3424.
(3) Schlick, S.; Kevan, L. *J. Chem. Phys.* **1980**, *72*, 784.
(4) Schlick, S.; Kevan, L. *J. Am. Chem. Soc.* **1980**, *102*, 4622.
(5) Campbell, R. F.; Freed, J. H. *J. Phys. Chem.* **1980**, *84*, 2668.
(6) Shiotani, M.; Moro, G.; Freed, J. H. *J. Chem. Phys.* **1980**, *74*, 2616.
(7) Ard, W. B.; Shields, H.; Gordy, W. *J. Chem. Phys.* **1955**, *23*, 1727.
(8) Schneider, E. E. *J. Chem. Phys.* **1955**, *23*, 978.
(9) Molin, Yu. N.; Tsvetkov, Yu. D. *Zh. Fiz. Khim.* **1959**, *33*, 1668.
(10) Matsugashita, T.; Shinohara, K. *J. Chem. Phys.* **1961**, *35*, 1652.
(11) Tanaka, H.; Matsumoto, A.; Goto, N. *Bull. Chem. Soc. Jpn.* **1964**, *37*, 1128.
(12) Ovenall, D. W. *J. Phys. Chem. Solids* **1965**, *26*, 81.
(13) Siegel, S.; Hedgpeth, H. *J. Chem. Phys.* **1967**, *46*, 3904.
(14) Rexroad, H. N.; Gordy, W. *J. Chem. Phys.* **1959**, *30*, 399.
(15) Iwasaki, M.; Sakai, Y. *J. Polym. Sci., Polym. Phys. Ed.* **1968**, *6*, 265.
(16) Milinchuk, V. K.; Klinshpont, E. R. *J. Polym. Sci., Polym. Symp.* **1973**, *40*, 1.
(17) Olivier, D.; Marachi, C.; Che, M. *J. Chem. Phys.* **1979**, *71*, 4688.
(18) Olivier, D.; Marachi, C.; Che, M. *J. Chem. Phys.* **1980**, *72*, 3348.
(19) Toriyama, K.; Iwasaki, M. *J. Phys. Chem.* **1969**, *73*, 2663.

0002-7863/82/1504-0668$01.25/0

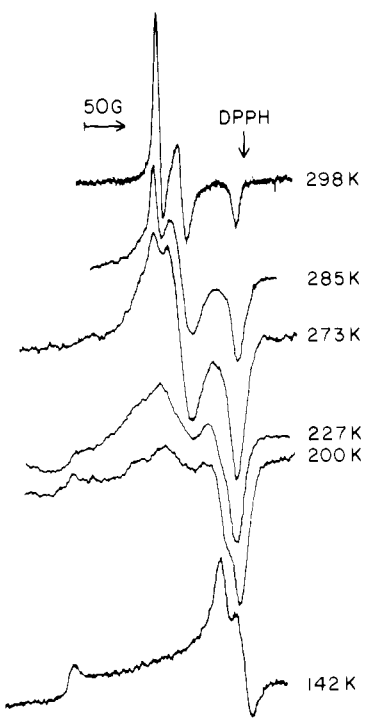

Figure 1. ESR spectra (35 GHz) of peroxy radicals in irradiated poly(tetrafluoroethylene) as a function of temperature.

radical (IV) the above sample containing both peroxy radicals III and IV was reevaculated for 24 h at room temperature to remove the oxygen. These samples were then UV irradiated at 77 K for about 1 h, using a 1000 W mercury lamp. Periodic ESR spectra were recorded on a Varian E-3 X-band ESR spectrometer to check the conversion of the peroxy mid-chain radical III to the end-chain radical II, perhaps via I. After essentially complete conversion to II, oxygen was introduced into the sample tubes to produce exclusively the peroxy end-chain radical IV.

The polycrystalline PTFE samples were compressed under 10 tons in a pellet press to make small pellets for Q-band ESR measurements. The ESR spectra were recorded on a Varian E-line Q-band spectrometer, operating at 35.0 GHz with 100 kHz magnetic-field modulation. Temperature variation was carried out by immersing the cavity in a dewar through which precooled nitrogen gas was circulated. The temperature inside the cavity was measured to ±5 °C, using a copper–constantan thermocouple with digital readout. Diphenylpicrylhydrazyl with g = 2.0036 was used as a g marker. The g values are accurate to ±0.0005. The magnetic-field sweep was calibrated with a Mn^{2+}-doped MgO sample, using a hyperfine coupling of 87.6 G.

Results

Q-Band ESR spectra measured on PTFE containing radical III, at 298, 285, 273, 227, 200 and 142 K, are shown in Figure 1. ESR spectra obtained at 298 K up to 365 K remain unchanged, although the spectral lines at 365 K are narrower than at 298 K. Similarly, the ESR spectra below 142 K to 77 K are practically the same. This suggests that the peroxy-radical motion is relatively "static" at 142 K and is "fast" at 298 K. The measured g values of the spectrum at 142 K are g_1 = 2.0394, g_2 = 2.0070, and g_3 = 2.0016, with g_{iso} = 2.0160. From the relative intensities of the spectrum at 142 K, one can conclude that $g_1 = g_{\parallel}$, and that g_2 and $g_3 \simeq g_{\perp}$.

For the ESR spectrum at 298 K in Figure 1 the g values are g_1^r = 2.0220, g_2^r = 2.0168, and g_3^r = 2.0055, giving g_{iso}^r = 2.0148 where superscript r represents room temperature. It is important to note that $g_{iso} \neq g_{iso}^r$ and the difference seems just outside experimental error. This discrepancy in the g values suggests that the 298 K spectrum might be composed of two radicals. It has been indicated from previous work that the peroxy mid-chain radical III has axially symmetric g values at room temperature,[15] whereas the peroxy end-chain radical IV spectrum has an isotropic g at 298 K.[17] Thus the g_i^r values are assigned as follows: radical III, $g_{\parallel}^{III} = g_3^r$ and $g_{\perp}^{III} = g_1^r$, $g_{iso}^{III} = g_{\parallel}^{III} + 2g_{\perp}^{III}$ = 2.0165; radical IV, $g_{iso}^{IV} = g_2^r$. Both g_{iso}^{III} and g_{iso}^{IV} are in agreement with the g_{iso} value at 142 K.

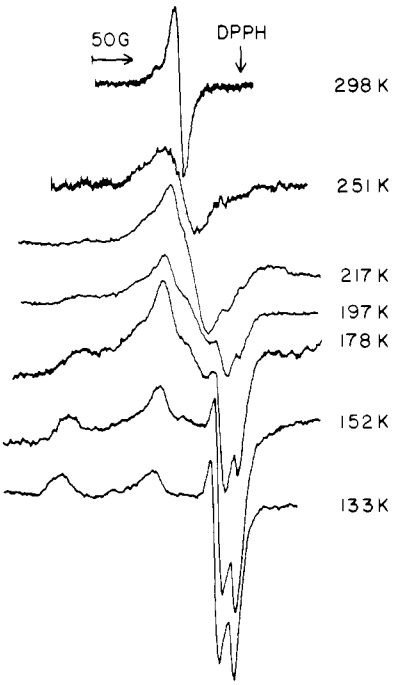

Figure 2. ESR spectra (35 GHz) of the peroxy end-chain radical IV in irradiated PTFE as a function of temperature.

The presence of radical IV in the room-temperature spectrum of Figure 1 has been suggested by earlier workers based on results with oriented PTFE samples.[12,15] To confirm this we produced the peroxy end-chain radical IV independently in PTFE samples as described above. The temperature variation in the Q-band ESR spectra of radical IV only is given in Figure 2. As seen from Figure 2, it is clear that radical IV exhibits complete g averaging at room temperature, yielding g_{iso}^{IV} = 2.0168. Complex line broadening in the spectra was observed at lower temperatures. However, at 77 K a rigid limit spectrum (as in Figure 1) is observed.[12]

In Figure 1, an isotropic line (near g_{iso}) which belongs to radical IV is evident in most of the experimental ESR spectra. The resultant ESR spectra obtained after subtracting the radical IV spectra are shown in Figure 3. From Figures 2 and 3, it is evident that "extra" lines occur for the peroxy radical III and IV at magnetic fields between g_1 and g_2 at intermediate temperatures. These are attributed to motional effects.

In the $Ph_3COO\cdot$ radical, such "extra" lines were reported and were attributed to the rotation of the O–O group around the C–O bond.[2] Also, in the case of peroxy radicals observed in the urea–polyethylene complex such extra features were ascribed to partial averaging of the g tensor by internal rotation of the O–O group about the C–O bond.[4] It was also pointed out that chain-axis rotation by 90° jumps also yields similar features in the peroxy-radical spectra.[4]

Here we apply a motional interpretation to the ESR spectra of peroxy radicals in PTFE. We consider the following specific motional models: (a) cubic jump model, (b) O–O group rotation around the C–O bond by two 180° jumps or three 120° jumps, and (c) chain-axis rotation by two 90° jumps or three 120° jumps.

Spectral Simulations. The spectral dependences as a function of jump rate τ^{-1} have been calculated using the formalism of the modified Bloch equations.[20] The polycrystalline ESR spectral line shape is written as

(20) Sullivan, P. D.; Bolton, J. R. "Advances in Magnetic Resonance"; Academic Press: New York, 1970; Vol. 4, pp 39–85.

$$Y(N,\tau) = \sum_{\theta=0°}^{\pi/2} \sum_{\phi=0°}^{\pi} G(\theta,\phi,\tau,N) \sin\theta \tag{1}$$

The general solution, G, for the total complex magnetization is obtained for a system with N sites, when all interconversion rates between the sites are equally probable. The solution G is written as[20]

$$G(\theta,\phi,\tau,N) = i\gamma H_1 M_0 \tau \sum_{s=1}^{N} f_s [N(1 - \sum_{s=1}^{N} f_s)]^{-1} \tag{2}$$

with

$$f_s = [N + \alpha_s \tau]^{-1} \tag{3}$$

and

$$\alpha_s = (T_{2s})^{-1} - i(\omega_s - \omega) \tag{4}$$

In eq 2, γ is the gyromagnetic ratio, H_1 is the microwave magnetic field, τ is the mean lifetime of any species in the system, $(T_{2s})^{-1}$ is the average line width of species s in the absence of motional effects, M_0 is the magnetization of the species along z in the absence of saturation, ω is the sweep of the spectrum in frequency units, and ω_s is the resonance frequency of species s. For the peroxy radicals we have only g anisotropy, and ω_s for a single orientation in θ and ϕ space is written

$$\omega_s = \left(\frac{\beta H}{\hbar}\right)\left[(l_1, l_2, l_3)\ \tilde{g}(s) \begin{pmatrix} l_1 \\ l_2 \\ l_3 \end{pmatrix}\right] \tag{5}$$

with the direction cosines l_1, l_2, and l_3 given by

$$l_1 = \sin\theta\cos\phi,\ l_2 = \sin\theta\sin\phi, \text{ and } l_3 = \cos\theta \tag{6}$$

In eq 5, H_0 represents the magnetic field at the center of the spectrum, β is the Bohr magneton, h is Planck's constant, and $\tilde{\mathbf{g}}(s)$ represents the $\mathbf{g}$ tensor for site s. For a "cubic-jump" process, the axes of the three sites (s = 1, 2, and 3) are interchanged by rotation about a body diagonal of a cube. Hence the $\tilde{\mathbf{g}}(s)$ are written as

$$\tilde{g}(1) = \begin{pmatrix} g_1 & 0 & 0 \\ 0 & g_2 & 0 \\ 0 & 0 & g_3 \end{pmatrix},\ \tilde{g}(2) = \begin{pmatrix} g_2 & 0 & 0 \\ 0 & g_3 & 0 \\ 0 & 0 & g_1 \end{pmatrix},\ \tilde{g}(3) = \begin{pmatrix} g_3 & 0 & 0 \\ 0 & g_1 & 0 \\ 0 & 0 & g_2 \end{pmatrix} \tag{7}$$

In the case of a C–O bond rotational model, the C–OO fragment is assumed to be perpendicular to the chain axis and the rotation takes place about the y' axis (see Figure 4a). Then $\tilde{\mathbf{g}}(s)$ is written as

$$\tilde{\mathbf{g}}(s) = \tilde{\mathbf{L}}_\rho \tilde{\mathbf{g}}(1) \tilde{\mathbf{L}}_\rho^{-1} \tag{8}$$

where $\tilde{\mathbf{L}}_\rho$ represents the transformation matrix of $\tilde{\mathbf{g}}_A(1)$ in a new coordinate system and

$$\rho = (s - 1)\epsilon \tag{9}$$

where ϵ represents the jump angle of value π/N or $2\pi/N$. That is, for a two-jump model, N = 2, ϵ can take values of 90 or 180°, and for a three-jump model, N = 3, ϵ will be 60° or 120° and so on.

For the C–O bond rotational model the elements of $\tilde{\mathbf{L}}_\rho$ are written as[2] in eq 10.

$$\tilde{L}_p = \begin{pmatrix} \cos^2\alpha\cos\rho + \sin^2\alpha & \sin\alpha\cos\rho\cos\alpha - \cos\alpha\sin\alpha & -\sin\rho\cos\alpha \\ \cos\alpha\sin\alpha\cos\rho - \sin\alpha\cos\alpha & \sin^2\alpha\cos\rho + \cos^2\alpha & -\sin\rho\sin\alpha \\ \cos\alpha\sin\rho & \sin\alpha\sin\rho & \cos\rho \end{pmatrix} \tag{10}$$

In eq 10, the parameter α represents the COO bond angle by the relation

$$\alpha = \angle COO - 90° \tag{11}$$

TEFLON PEROXY MID-CHAIN RADICAL Q-BAND

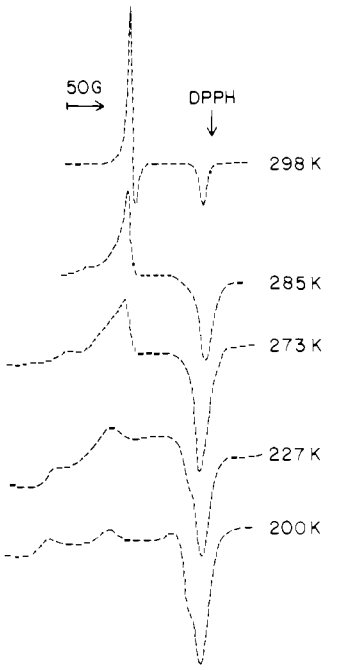

Figure 3. The resultant ESR spectra of mid-chain peroxy radical III after subtracting end-chain radical IV from Figure 1.

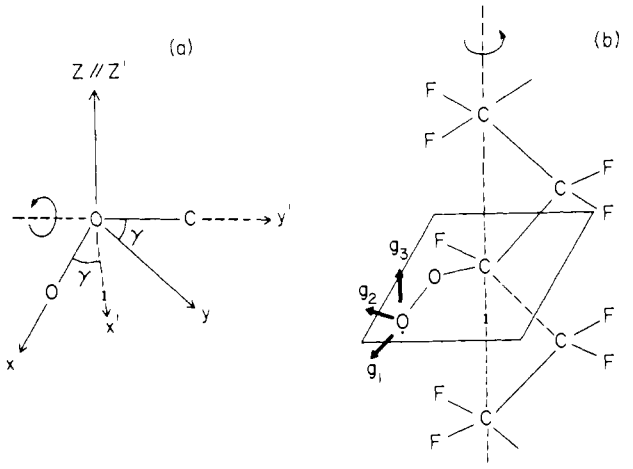

Figure 4. (a) Molecular axes x, y, z of the g tensor of the COO group and their orientation with respect to the C–O bond. Axes x',y',z' represent a new coordinate system obtained after rotating by an angle γ about z. (b) Schematic representation of the O–O group orientation relative to the PTFE molecular chain axis.

In the case of rotation about the chain axis, the rotation is assumed to take place about the z axis (see Figure 4b), and $\tilde{\mathbf{L}}_\rho$ is written as

$$\tilde{L}_p = \begin{pmatrix} \cos\rho & \sin\rho & 0 \\ -\sin\rho & \cos\rho & 0 \\ 0 & 0 & 1 \end{pmatrix} \tag{12}$$

Equation 12 is the rotation operator R_z.[21] In the case of eq 10, the rotation about the y' axis (see Figure 4) is a product of $(R_z R_{y'} R_z^{-1})$.[21]

Spectra were calculated, using eq 1–12, for the three different models: cubic jump, C–O bond rotation, and chain-axis rotation. The rate of interconversion between sites, τ^{-1}, is of the order of the frequency sprread of the spectrum which is ~300 G or ~840

(21) Tinkham, M. "Group Theory and Quantum Mechanics"; McGraw-Hill: New York, 1964; Chapter 5.

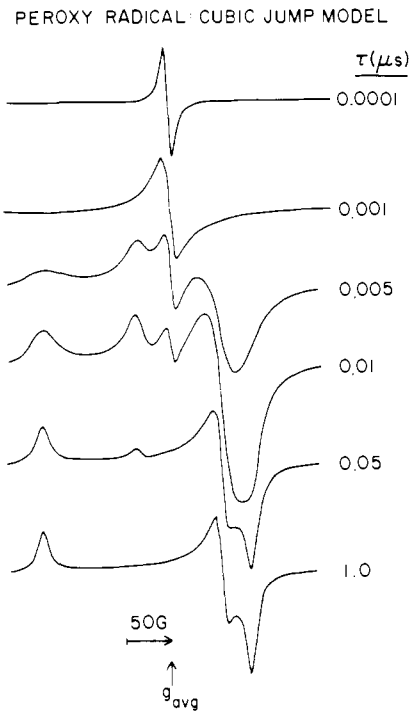

Figure 5. Simulated ESR powder spectra obtained by assuming "cubic" jumps as a function of correlation time, τ. g_{av} represents the field position of the average value of the principal g values. A line width of 15 MHz is used at $\tau = 0.0001$ μs, whereas a 20 MHz line width is employed for the rest of the spectra in order to get the best fit.

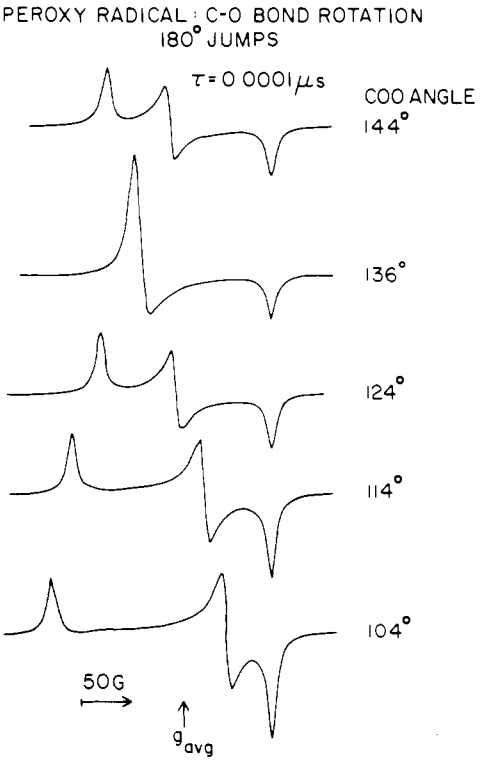

Figure 6. Simulated ESR powder spectra obtained by assuming a jump angle of 180° about the CO bond as a function of the COO angle with $\tau = 0.0001$ μs and an intrinsic line width of 15 MHz.

MHz. Spectral changes are expected to occur for $\gamma \leq 5 \times 10^{-9}$ s. The parameter τ was varied between 10^{-6} and 10^{-10}_{s} in appropriate intervals. The g tensors corresponding to the "rigid" limit experimental spectrum are designated as the elements of $\tilde{\mathbf{g}}(1)$. These are used in all the simulations to calculate g-tensor elements for various sites. The other parameter that is needed for the simulation is the line width $(T_{2s})^{-1}$ in the absence of site interconversion. Values of 15–20 MHz for $(T_{2s})^{-1}$ were used on the basis of a comparison of calculated and experimental spectra in the limit of high and low temperatures.

With regard to the variable N, two-jump as well as three-jump processes were considered for the C–O bond and the chain-axis rotation models. A jump angle ϵ of 90° or 180° was used for the two-jump process, and 60° or 120° was used for the three-jump process.

(a) Cubic-Jump Model. The spectral simulations for the cubic-jump model are given in Figure 5 as a function of τ. The simulations yield an isotropic spectrum under "fast" interconversion rates, $\tau^{-1} \simeq 10^{10}$ s^{-1}, between the three sites. For $\tau^{-1} = 10^{6}$ s^{-1}, a "rigid limit" spectrum is observed. At "intermediate" interconversion rates, $10^{9} > \tau^{-1} > 10^{7}$ s^{-1}, two partially resolved "extra" lines are observed near the g_{av} region of the spectra whose intensities montonically decrease near the rigid limit. These features found in the calculated spectra compare very well with those of the experimental spectra for the peroxy end-chain radical IV (see Figure 3). The field positions as well as the relative intensities of the "extra" lines are well reproduced in the simulated spectra for the entire temperature range. Other motional models involving C–O bond or chain-axis rotation do not reproduce the experimental data. Hence, we suggest that the peroxy end-chain radical IV undergoes a cubic-jump motional process.

In the case of the peroxy mid-chain radical III, the cubic-jump model fails, since the axiality in the observed spectra of III at 298 K (see Figure 4) is not reproduced. Hence we consider the following motional models.

(b) C–O Bond Rotation Model. Spectra simulations for the C–O bond rotation model, using a 180° two-jump process, are given in Figures 6 and 7. Simulated spectra for 180° jumps are very sensitive to the value of the COO bond angle according to eq 10 and 11. The spectral variations with the COO bond angle obtained for a constant value of $\tau = 10^{-10}$ s are given in Figure 6. From Figure 6 it is clear that an axial g tensor similar to the experimental result at 298 K (see Figure 3) is observed only for a COO bond angle of 136°.

Various values for the COO bond angle ranging between 104° [19] and 135° [2] are reported in the literature for peroxy radicals. For a COO bond angle of 104° a rigid limit spectrum even at $\tau = 0.0001$ μs is obtained as shown in Figure 6. Thus, this motional model can only give a satisfactory simulation for bond angles much greater than 104°. With use of a COO bond angle of 136°, simulated spectra for 180° jumps, for τ between 1.0 and 0.0001 μs, are given in Figure 7. Simulations with two 180° jumps reproduce most of the salient features of the experimental spectra in Figure 3. The axiality at 298 K and the one "extra" line occurring near $g_{\perp}^{r}$ at intermediate temperatures are satisfactorily reproduced.

For comparison, we have performed simulations where the O–O group undergoes three discrete jumps of 120° about the C–O bond in Figure 8 again assuming a COO bond angle of 136°. These simulations show a quite different averaging than found experimentally. At fast interconversion rates ($\tau^{-1} = 10^{10}$ s^{-1}) the calculated spectrum has wrong line positions and relative intensities. Hence a three-jump or any higher-jump ($N > 3$) process for the C–O bond rotation model does not seem to fit the motional mechanism for radical III.

It appears that a 180° jump C–O bond rotation model will account for the motional spectra of the mid-chain peroxy radical III *if* a COO bond angle of 136° can be justified. However, there is one aspect of the simulated spectra that does not agree with experiment, namely the position of $g_{\parallel}^{r}$. In the simulations the position of g_3 (g_{zz}) remains unchanged as τ is increased from a rigid limit value because any rotation in the xy plane does not change the value along z. thus the calculated $g_{\parallel}^{r}$ component is 2.0016 whereas the experimental value at 298 K is 2.0055 (see Figure 3). This discrepancy might be due to the presence of other motional effects.

Toriyama and Iwasaki[19] studied motional effects of trifluoroacetamide peroxy radical, $\cdot OOCF_3CONH_2$, at 77 and 300 K. They considered a case where the internal rotation of the O–O bond occurs simultaneously with C–O bond rotation. They give

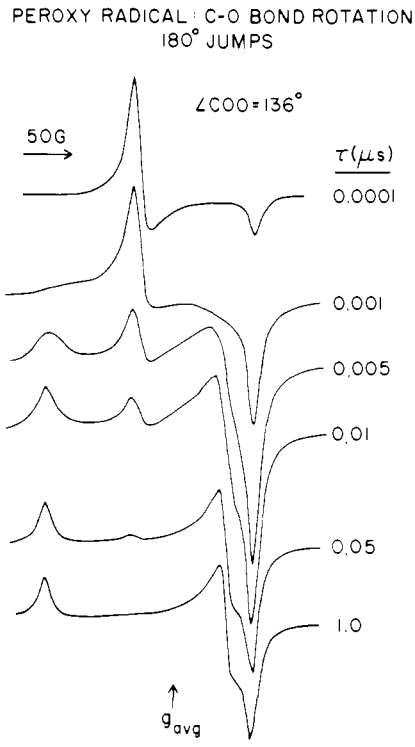

Figure 7. Simulated ESR powder spectra obtained by assuming a C–O bond rotation with two 180° jumps, as a function of τ. The line width in the absence of intramolecular motion is 20 MHz.

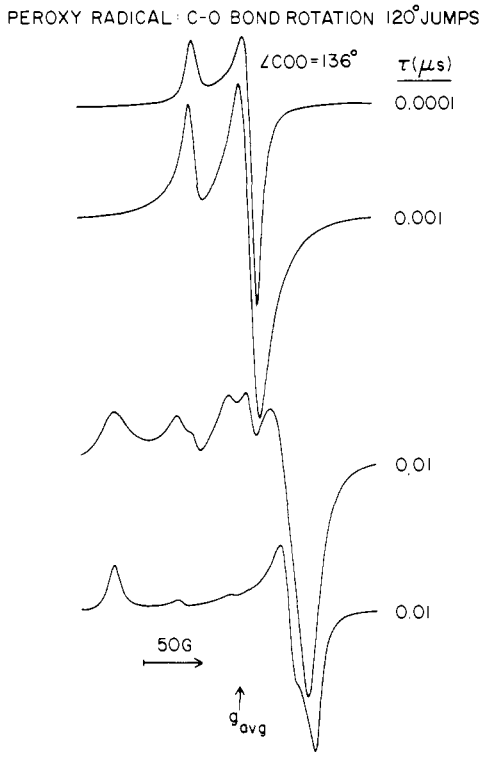

Figure 8. Simulated ESR powder spectra obtained by assuming a C–O bond rotation, with three 120° jumps, as a function of τ. The COO angle is 136° and the line width is 20 MHz in the absence of intramolecular motions.

empirical relations for averaging the g tensor at an arbitrary direction in the molecular axes system which are given here.[19]

$$g_{\parallel}^{rot} = 1/2(g_1 + g_2) \sin^2 \theta + g_3 \cos^2 \theta$$

$$g_{\perp}^{rot} = 1/2[(g_1 + g_2 + g_3) - g_{\parallel}^{rot}]$$

Using a complementary angle $\theta = 76°$, which corresponds to a COO bond angle of 104°, one obtains $g_{\parallel}^{rot} = 2.0064$ and $g_{\perp}^{rot}$ = 2.0208. these values of $g_{\parallel}^{rot}$ and $g_{\perp}^{rot}$ are close to our experimental values of $g_{\parallel}^{r}$ (2.0055) and $g_{\perp}^{r}$ (2.022) at 298 K for radical III. However, this suggests a much smaller COO bond angle of 104° compared to 136° used in the relative successful simulations with the 180° jump C–O bond rotation model. If the smaller bond angle is correct, then the CO bond rotation model does not fit the experimental data and we must explore other motional mechanisms.

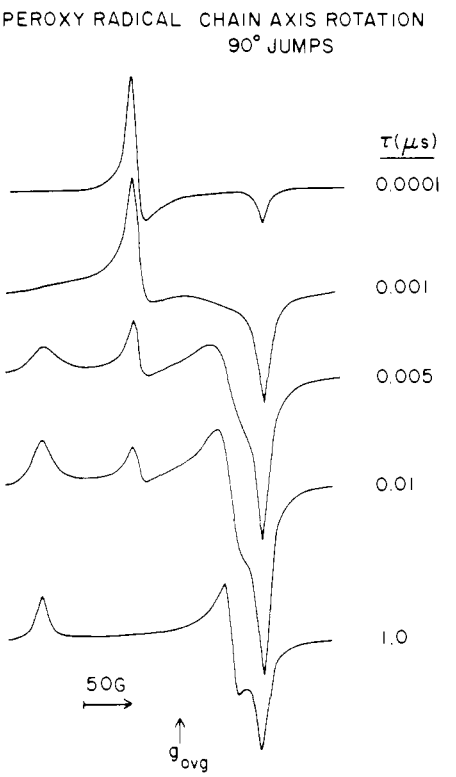

Figure 9. Simulated ESR powder spectra obtained by assuming a jump angle of 90° about the PTFE chain azis as a function of τ. The line width in the absence of motion is 20 MHz.

(c) Chain-Axis Rotation Model. In this model we assume discrete jumps of the O–O group about the PTFE chain axis as shown schematically in Figure 4b. Simulations were performed using eq 1–12 and the calculated spectra are given in Figures 9 and 10 for two-jump and three-jump processes, respectively. In the two-jump process we considered a jump angle of 90° instead of 180°, since a 180° rotation about the z axis leaves the g tensor unaltered as seen from eq 12. Figure 9 illustrates the spectral dependences as a function of τ calculated in the range between 10^{-6} and 10^{-10} s, at $\tau = 10^{-6}$ s, the simulated spectrum coincides with the experimental rigid limit spectrum observed at 142 K. Under fast interconversion rates with $\tau^{-1} = 10^{10}$ s^{-1} the calculated spectrum shows an axial g tensor with the same line shape as observed experimentally in Figure 3. At intermediate τ values between 10^{-9} and 10^{-7} s a single "extra" line is noticed whose position coincides with $g_{\perp}^{r}$ at 298 K and whose intensity decreases monotonically as the τ value approaches the rigid limit at 10^{-6} s. These features are practically the same as observed in the simulated spectra using the C–O bond rotation model with two 180° jumps and a COO bond angle of 136°. In the chain-axis rotation model, the calculated position of g_3^r remains unchanged for any value of τ since rotation is assumed about the z axis.

For comparison, the simulated spectra for chain-axis rotation via a three-jump process with 120° jump angles are given in Figure 10. This shows two "extra" lines instead of one "extra" line which disagrees with experiment. Hence the higher jump processes ($N \geq 3$) are not considered.

Discussion

It is interesting that the end-chain and mid-chain peroxy radicals in PTFE show quite different motional mechanisms. This is likely

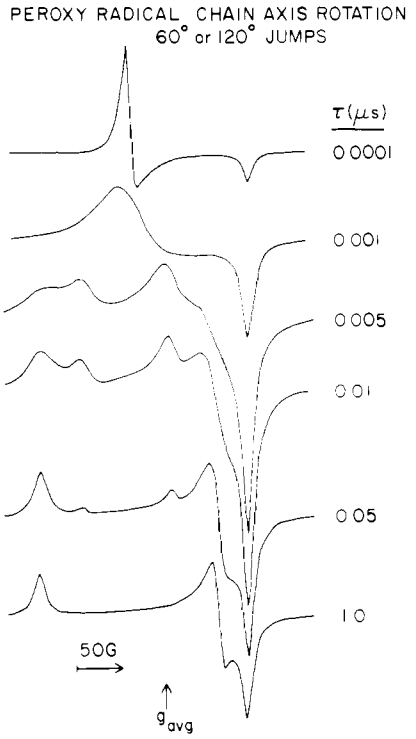

Figure 10. Simulated ESR powder spectra obtained by assuming a jump angle of 120° about the PTFE chain axis as a function of τ. The line width in the absence of intramolecular motion is 20 MHz.

related to differences in their environmental flexibility. The end-chain peroxy radical spectra are nicely consistent with a cubic-jump motional model. This type of motion seems possible for a small peroxy radical[3] or for an end-chain peroxy radical with sufficient flexibility.

The mid-chain peroxy radical is more constrained in its motion. From the simulation both C–O bond rotation and chain-axis rotation models seem to fit its temperature-dependent spectra. However, the C–O bond rotation model only fits for the specific COO bond angle near 136° and this does not seem consistent with inclusion of a subsidiary O–O bond rotation to explain the experimental position of $g_{\parallel}^{r}$. The chain-axis rotation model is not sensitive to the COO bond angle and thus is consistent with a subsidiary O–O bond rotation. We thus conclude that a specific motional mechanism involving chain-axis rotation fits best.

Additional evidence for a subsidiary O–O bond rotation is found from the "best" spin packet widths, $(T_{2s})^{-1}$, assumed in the simulations. The simulations were distinctly better when a homogeneous packet width of 15 MHz was used at room temperature and a broader width of 20 MHz was used at lower temperatures. The narrower packet width at room temperature may reflect additional averaging by another motional mechanism which could be O–O bond rotation for the mid-chain peroxy radical.

The chain-axis rotation mechanism is supported by other findings. The precursor to the mid-chain peroxy radical is the fluoroalkyl radical $-CF_2-\dot{C}F-CF_2-$ (I) which exhibits motional effects in its ESR spectrum which can only be interpreted due

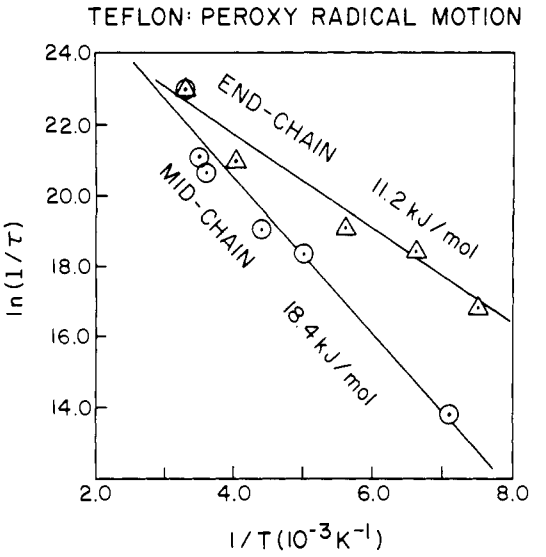

Figure 11. Arrhenius plots of the jump rate ln $(^1/\tau)$ as a function of T^{-1}. The lines are obtained by a linear least-squares fit, using the expression: ln $(1/\tau)$ – ln $(1/\tau) - E_a/RT$, where $1/\tau_0 = 6.141 \times 10^{12}$ s^{-1} and E_a = 18.4 kJ/mol for the mid-chain peroxy radical and $1/\tau_0 = 5.08 \times 10^{11}$ s^{-1} and E_a = 11.2 kJ/mol for the end-chain peroxy radical.

to chain-axis motion.[22] In oriented samples of PTFE it has been shown that a broad nuclear magnetic resonance component shows line broadening near 290 K.[23] This was ascribed to the onset of rotational motion of the molecular chains in crystalline regions. Rotation transition phenomena have also been observed from the temperature dependence of the X-ray diffraction patterns. Hori et al.[25] have very recently studied the temperature dependence of ESR spectra for peroxy mid-chain radicals in oriented crystals of the urea–*n*–tetracosane complex and have concluded that the motion involves chain-axis rotation.

The barrier heights for the motional processes deduced have been determined by fitting an Arrhenius temperature dependence. We have used the expression

$$\ln (1/\tau) = \ln (1/\tau_0) - E_a/RT \qquad (13)$$

where E_a is the activation energy, R is the gas constant, and τ_0^{-1} is the frequency factor. Figure 11 shows a plot of ln $(1/\tau)$ vs. $1/T$ for the mid-chain peroxy radical which fits eq 13 well. From a least-squares fit of the data points a barrier height of 18.4 kJ/mol is obtained. Similarly a barrier height of 11.2 kJ/mol is found for the end-chain peroxy radical. These values of barrier heights are close to those reported for other peroxy radicals.[2-4]

Acknowledgment. We thank the Army Research Office for support of this research.

Registry No. Poly(tetrafluoroethylene), 9002-84-0.

(22) Tamura, N. *J. Chem. Phys.* **1961**, *37*, 479.
(23) Hyndman, D.; Origlio, G. F. *J. Appl. Phys.* **1960**, *31*, 1849.
(24) Bunn, C. W.; Howells, E. R. *Nature (London)* **1954**, *174*, 549.
(25) Hori, Y.; Aoyama, S.; Kashiwabara, H. *J. Chem. Phys.* **1981**, *75*, 1582.